

A Spectroscopic Investigation of Hydrogen Bond Patterns in Crystalline and Amorphous Phases in Dihydropyridine Calcium Channel Blockers

Xiaolin Charlie Tang,¹ Michael J. Pikal,¹ and Lynne S. Taylor^{2,3}

Received December 6, 2001; accepted January 4, 2002

Purpose. To gain insight into the molecular structure of amorphous compounds by investigating hydrogen bonding patterns and strength in a series of structurally related compounds. Seven 1,4-dihydropyridine calcium channel blockers were evaluated.

Methods. FT-Raman and FT-infrared spectra of the compounds in the crystalline and amorphous states were obtained.

Results. For crystalline compounds, the position of the NH vibration varied considerably, indicating that the strength of hydrogen bonding differs between the different compounds in agreement with published single crystal X-ray data. For the amorphous phases, the NH vibration occurred at approximately the same position for all compounds, suggesting a uniform average hydrogen bonding strength. Somewhat surprisingly, for some compounds, the average hydrogen bond strength in the amorphous state was found to be greater than in the crystalline compound, although for others, it was weaker as anticipated. Hydrogen bonding patterns (acceptor group) varied between the crystalline compounds, but were remarkably consistent in the amorphous compounds; thus the acceptor group in the amorphous phase is not necessarily the same as in the crystalline counterpart.

Conclusions. Hydrogen bond patterns and strength within a group of chemically related amorphous compounds were found to be very similar, but were different from those in the equivalent group of crystalline substances.

KEY WORDS: crystalline; amorphous; hydrogen bonding; vibrational spectroscopy.

INTRODUCTION

During crystallization, molecules become arranged into a three dimensionally ordered phase. The arrangement of the molecules represents a local minimum in free energy. By extensive analysis of X-ray diffraction data obtained from crystals, rules have been developed, which describe the factors that appear to be important in determining the ordering of molecules (1). Firstly, it has been observed that molecules pack so that free volume is minimized and hence density is maximized. This has been termed Kitagorodski's rule of close packing. Secondly, analysis of hydrogen bonding patterns has revealed a tendency for the best hydrogen bond donors to interact with the best acceptor groups (2). Thirdly, electrostatic repulsions are minimized.

Amorphous materials are fundamentally very different from their crystalline counterparts. They are difficult both to define thermodynamically and to analyze structurally. Due to their lack of long-range three-dimensional order, they cannot easily be analyzed by X-ray diffraction techniques. Thus information about the arrangement of the molecules relative to one another and the nature of any intermolecular interactions is not readily obtained. Neutron scattering has been used to study the structure of amorphous glucose (3), however this technique is not widely available. Optical spectroscopy has been used extensively to gather structural information on glasses (4).

As a result of their widespread occurrence, it is of interest to understand more about the molecular structure of amorphous materials and how they differ from their crystalline counterparts. It can be anticipated that intermolecular interactions are important in determining not only the properties of an amorphous phase but also those of molecular level amorphous mixtures such as lyophilized systems and solid dispersions. Indeed, there have been a number of reports describing interactions in binary systems (5–9). Amorphous materials are metastable relative to the crystalline state, hence phase transformation may occur. An understanding of molecular associations in amorphous compounds and how they differ from those in the corresponding crystal should provide a more in-depth understanding of the tendency for crystallization and how this can be prevented by selection of appropriate crystallization inhibitors. The purpose of this study was to investigate hydrogen-bonding interactions in single component amorphous phases and to compare and contrast these interactions with those found in the crystalline counterparts. Infrared (IR) and Raman spectroscopy were used as analytical tools to detect these interactions, techniques well established for this purpose (10). A selection of 1,4 dihydropyridine calcium channel blockers, used to lower blood pressure, were chosen as model compounds. The structures of these compounds are shown in Fig. 1. Each contains an identical core structure, also shown in Fig. 1 but are substituted differently at various positions, providing a sufficient degree of both chemical similarity and diversity. Moreover, the single crystal structure of five of these substances has been published.

MATERIALS AND METHODS

Felodipine was obtained from AstraZeneca, Södertälje, Sweden. Nifedipine, nifedipine hydrochloride, nitrendipine, and nimodipine were purchased from Göteborgs Termometerfabrik AB, Sweden. Isradipine and nisoldipine were kindly supplied by Novartis AG (Basel, Switzerland) and Bayer AG (Wuppertal, Germany), respectively. Nifedipine hydrochloride (HCl) was converted to the free base by reaction with NaOH. The HCl salt was dissolved in water and an excess of NaOH was added. The free base has a very low solubility in water and separated out as a film, which was washed with water and then dissolved in ethanol. Following evaporation of ethanol, an amorphous phase was produced, which with time formed a partially crystalline phase.

Amorphous phases of all compounds were prepared by heating the crystalline substance, in a suitable container, up to just above the melting point and holding for 1 min followed by quenching of the container in cold water or on a metal

¹ School of Pharmacy, U-2092, University of Connecticut, 372 Fairfield Road, Storrs, Connecticut 06296-2092.

² Solid State Analysis, Pharmaceutical and Analytical R&D, AstraZeneca R&D Mölndal, S-431 83 Mölndal, Sweden.

³ To whom correspondence should be addressed. (e-mail Taylor@Astrazeneca.com)

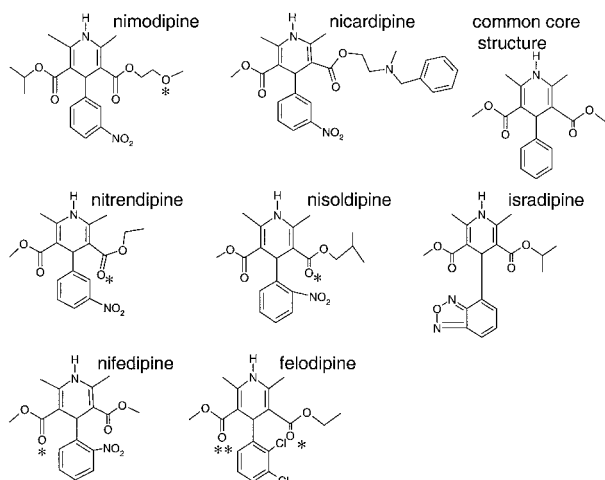


Fig. 1. Structures of the compounds whereby * indicates the acceptor group involved in a hydrogen bond and ** indicates where a second acceptor group is involved in hydrogen bonding. The acceptor groups were determined from published single crystal data.

surface. No visible signs of degradation were observed and for felodipine, the purity of the amorphous sample was checked with high performance liquid chromatography. The purity following the melting procedure was greater than 99.9%. Samples were analyzed immediately after being made amorphous. Care was taken to avoid contamination of samples with water vapor. All of the compounds have extremely low water solubility, and hygroscopicity of the amorphous phase was not found to be a problem over the time scale of sample preparation [exposure to atmospheric humidity (around 40% relative humidity) for less than 5 m]. Samples for Raman spectroscopy were prepared by melting directly in nuclear magnetic resonance (NMR) tubes followed by sealing of the tubes. Samples for IR spectroscopy were loaded into the nitrogen atmosphere of the instrument immediately after sample preparation.

FT-Raman Spectroscopy

FT-Raman spectra were collected on a Perkin-Elmer System 2000 instrument (Beaconfield, United Kingdom) with a near infrared Nd:YAG laser operating at 1064 nm. The laser power was typically 500 mW and an InGaAs detector was used. Back-scattered radiation at an angle of 180° was collected and the Stokes radiation reported. Indene was used as a reference standard to monitor wavenumber accuracy. Two hundred fifty-six scans at a resolution of 2 cm⁻¹ were averaged for each sample. Samples were analyzed in sealed NMR tubes with continuous rotation.

FT Infrared Spectroscopy

Infrared spectra were obtained using a Biorad FTS 575C spectrometer (Kent, United Kingdom) equipped with a KBr beamsplitter and a Peltier cooled DTGS detector. The sample and optics compartment were purged with dry nitrogen. Spectra were obtained either from KBr discs containing between 0.5–1% of drug or by using an attenuated total reflection (ATR) accessory (diamond crystal, Golden Gate, Graseby Specac, Inc.). Transmission spectra were obtained from the KBr discs at a resolution of 2 cm⁻¹, and a resolution of 4 cm⁻¹ was used for the ATR accessory. Between 64 and 256 scans were acquired. The ATR accessory was used to check that the

sample processing used to form KBr discs did not alter the sample. In all cases the ATR spectra were found to be comparable to the transmission spectra indicating that no sample transformation took place.

Theoretical Considerations

IR and Raman spectroscopy are used extensively to investigate hydrogen bonding because the peak position of the X-H stretch is very sensitive to the extent of association. The unbonded X-H stretch gives rise to a relatively sharp peak, whereas on formation of a hydrogen bond, X-H ··· Y (where Y is the acceptor atom), the peak shifts to a lower wave number and becomes much broader (11). The downward shift is caused by the lengthening of the X-H bond, which results on hydrogen bond formation. Hence a stronger hydrogen bond will lengthen X-H more and produce a shift to a lower wave number. Furthermore, a relationship between the peak position of the X-H group and the X-H ··· Y bond distance (determined from crystallographic data) has been observed, whereby a lower peak frequency correlates with a shorter hydrogen bond distance (i.e., stronger hydrogen bond and longer X-H bond) (12). In this study, the assumption is made that the NH peak position reflects the average hydrogen bond strength whereas the width of the peak gives some indication of the distribution of hydrogen bond energies (13). Because a plot of crystalline NH peak position vs. N ··· O distance (from single crystal measurements, see Table I) yielded a linear relationship (R² value of 0.974) as shown in Fig. 2, this assumption is reasonably valid.

When describing the strengths of hydrogen bonds, we have used the classification of Jeffrey whereby a moderate hydrogen bond has a H ··· Y distance of ~1.5–2.2 Å and a X-H ··· Y distance of ~2.5–3.2 Å, and weak hydrogen bonds have corresponding values of ~2.2–3.2 Å and ~3.2–4.0 Å, respectively (14).

RESULTS

Molecular structures of the model compounds are shown in Fig. 1. Each compound contains only one hydrogen bond donor, the dihydropyridine NH group. In contrast, a number of proton acceptors are present in each compound; typically carbonyl, ether and nitro functions, and the nitrogen in the dihydropyridine ring. The acceptor groups involved in hydrogen bonding in the crystalline samples are marked by an asterisk in Fig. 1 for 5 of the compounds (ascertained from published single crystal X-ray data), and Table I contains information about the lengths and angles of the hydrogen bonds (15–19). These data were used to aid assignment of the peaks in the IR and Raman spectra of the crystalline compounds. The spectra of the crystalline materials were then compared with their amorphous counterparts to try and elucidate the nature of the hydrogen bond interactions in the amorphous phase.

The IR and Raman spectra of crystalline and amorphous felodipine are shown in Fig. 3. A number of differences are immediately apparent. In addition to a broadening of peaks in the amorphous sample (particularly for the Raman spectra), changes in peak shape, intensity, and position have occurred. Peak positions and assignments for selected peaks of interest (those involved in hydrogen bonding) are shown in Table II for crystalline and amorphous phases. From Fig. 1 and Table I it can be seen that, in crystalline felodipine, there is hydro-

Table I. Hydrogen Bond Patterns and Properties for the Different Amorphous and Crystalline Compounds (For the crystalline materials, the hydrogen bond properties for the N–H···O interaction are taken from the published single crystal X-ray data where available. For structures where the hydrogen positions were not reported, the N···O distance is given, and for the structures where the hydrogens were reported, both the N···O and the H···O distances are noted, as is the angle for the N–H···O hydrogen bond interaction. The hydrogen bond acceptor is also marked on Fig. 1. For amorphous compounds and crystalline isradipine and nicardipine, the hydrogen bond acceptors were deduced from the spectroscopic data.)

Compound	H bond pattern	Distance and angle
Felodipine	Crystalline NH···O=C ^{b*}	3.155 Å (N···O*) 2.669 Å (H···O*), 119°
	Crystalline NH···O=C**	3.237 Å (N···O**) 2.43 Å (H···O**), 163°C
Nifedipine	Amorphous NH···O=C ^a	
	Crystalline NH···O=C	3.028 Å (N···O)
Isradipine	Crystalline NH···benzoxadiazole ^a	
	Amorphous NH···O=C ^a	
Nimodipine	Crystalline NH···O (ether)	2.835 Å (N···O)
	Amorphous NH···O=C ^a	
Nisoldipine	Crystalline NH···O=C	2.894 Å (N···O) 2.006 Å, 174° (H···O)
	Amorphous NH···O=C ^a	
Nitrendipine	Crystalline NH···O=C	2.892 Å (N···O) 2.115 Å, 165° (H···O)
	Amorphous NH···O=C ^a	
Nicardipine	Crystalline NH···O=C ^a	
	Amorphous NH···O=C ^a	
	Amorphous NH···O=C ^a	

^a Deduced from spectroscopic data only.

^{b*} and ^{**}see Fig. 1.

gen bonding between the NH group and both the methyl ester and ethyl ester carbonyl groups (16), although these hydrogen bonds are both longer than those found in the other compounds. The NH peak occurs at around 3370 cm⁻¹ (Fig. 4A) and there are two carbonyl peaks (Fig. 4B). The lower wavenumber peak at around 1690 cm⁻¹ can be assigned to the ethyl ester carbonyl, which is involved in the shorter hydrogen bond [hydrogen bond formation reduces the carbonyl peak position (11)] and the 1700 cm⁻¹ peak to the weakly hydrogen bonded methyl ester carbonyl.

From Fig. 4A and Table II, it can be seen that in amorphous felodipine, the NH peak is broader and has shifted by around 33 cm⁻¹ to a lower wave-number. There is a simultaneous change in the carbonyl region (Fig. 4B and Table II) in which one peak shifts downwards by 8 cm⁻¹, whereas the other peak shifts by 2 cm⁻¹ to a higher peak position. The downward shift in position of the NH group suggests that the average hydrogen bond in the amorphous phase is stronger than in the crystalline phase. The concomitant decrease in wave-number of one of the carbonyl groups supports this conclusion and also indicates that this is the acceptor group. Because only one carbonyl peak shifts downwards, whereas the other shifts slightly upwards, it can be inferred that in the amorphous phase only one of the carbonyls is hydrogen bonded, whereas the other is unassociated (or extremely weakly hydrogen bonded). In both the IR and Raman spectra of amorphous felodipine (Fig. 3), a small peak appears around 3420 cm⁻¹. This peak is thought to arise from a small fraction of non-hydrogen bonded NH, which is present in the amorphous material. Similar observations have been made for other amorphous materials (6,13), and the peak position is

within the range observed for non-bonded NH stretch in other systems (13,20)

A similar type of analysis of the spectral data was carried out for the other compounds, and the information and results are summarized in Tables I and II. Each compound will be briefly described.

In crystalline nifedipine, there is a medium strength hydrogen bonding interaction between the NH group and one of the methyl ester functionalities (15). The N···O interatomic distance (Table I) indicates that this interaction is somewhat shorter than in felodipine suggesting a stronger hydrogen

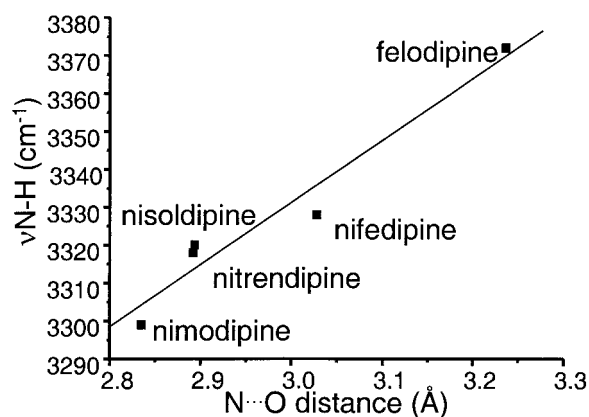


Fig. 2. Relationship between the N···O interatomic distance in the crystal and the NH stretching frequency is shown. The N···O distance was taken from published single crystal X-ray data. Linear regression analysis was performed and the R² correlation coefficient was 0.974.

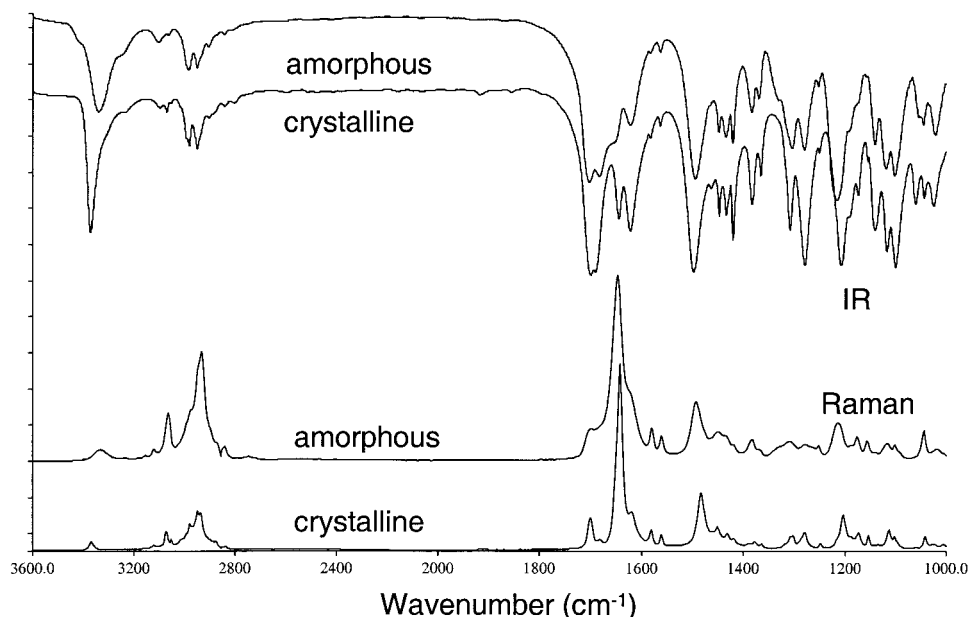


Fig. 3. Raman and IR spectra of crystalline and amorphous felodipine over the spectral range 3600–1000 cm^{-1} .

bond (assuming similar hydrogen bond geometry). The position of the NH vibration in crystalline nifedipine appears at a considerably lower wavenumber than in felodipine, supporting this supposition (Table II). Again two carbonyl peaks are observed, consistent with one hydrogen bonded and one non-hydrogen bonded group. On forming amorphous nifedipine, the NH vibration shifts upwards by 14 cm^{-1} , indicating that, in contrast to felodipine, the hydrogen bond strength decreases with loss of crystalline structure. The carbonyl peaks support this conjecture as both shift to higher wave numbers. It should also be noted that both the NH and the carbonyl peak positions are very similar to those in amorphous felodipine. There was no evidence to suggest that other potential acceptor groups play a major role in hydrogen bonding in the amorphous phase (data not shown).

The hydrogen bonding patterns in crystalline nisoldipine and nitrendipine are similar to those observed for nifedipine (Fig. 1, Table I). Both compounds have shorter hydrogen bonds than either felodipine or nifedipine, and NH peak positions are consequently lower. On forming the amorphous phases, the NH peak position increased in both cases, suggesting reduced hydrogen bond strength. The positions of the carbonyl peaks are very similar to those of the other amorphous compounds implying similar hydrogen bond patterns and strengths (Table II).

In crystalline nimodipine the hydrogen bond is between the NH and the ether oxygen (Fig. 1) (17). The $\text{N} \cdots \text{O}$ distance is the shortest of all the compounds suggesting that the hydrogen bond may be stronger in crystalline nimodipine than in the other compounds. The IR/Raman data of crystalline nimodipine supports this hypothesis because the NH stretch is found at the lowest wave number position for all the compounds, at 3299 cm^{-1} . The carbonyl peaks are found at relatively high wave numbers, 1700 and 1693 cm^{-1} , as would be expected given their non-hydrogen bonded status. In the amorphous spectrum, the NH peak shifts upwards by around 35 cm^{-1} whereas one of the carbonyls shifts downwards by 14 cm^{-1} . These results indicate that hydrogen bond strength de-

creases in the amorphous state and the hydrogen bond acceptor changes from the ether oxygen to one of the carbonyl groups. This is supported by the observation that the C–O stretching peak also undergoes a substantial shift in peak position on changing from the crystalline and amorphous phase (it shifts upwards by 12 cm^{-1} on changing from crystalline to amorphous).

Table II. IR and Raman Peak Positions for the NH and C=O Stretching Vibrations for the Various Crystalline and Amorphous Compounds

Compound	$\nu\text{NH} (\text{cm}^{-1})$		$\nu\text{C}=\text{O} (\text{cm}^{-1})$	
	Crystalline	Amorphous	Crystalline	Amorphous
Felodipine				
IR	3372	3339	1699, 1690	1701, 1682
Raman	3371	3335	1702, 1683	1700, ^a
Nifedipine				
IR	3328	3342	1689, 1680	1703, 1684
Raman	3330	3332	1679 ^b	1704, 1680 ^c
Isradipine				
IR	3349	3341	1703	1699, 1680
Raman	3349	3335	1698	1699, 1682 ^c
Nimodipine				
IR	3299	3338	1700, 1693	1696, 1677
Raman	3299	3328	1698, 1692 ^c	1700, 1679
Nisoldipine				
IR	3321	3341	1706	1697, 1680
Raman	3322	3336	1700, 1670	1701, 1679 ^c
Nitrendipine				
IR	3318	3338	1701 ^a	1702, 1682
Raman	3318	3326	1699, 1666	1702, 1682
Nicardipine				
IR	3354	3339	1702, 1683	1698, 1680
Raman			—	1701, 1682

^a Peak too broad to be measured or not sufficiently resolved from a neighbouring peak.

^b On cooling, this peak resolved into two.

^c Indicates peak was a shoulder to a neighboring peak.

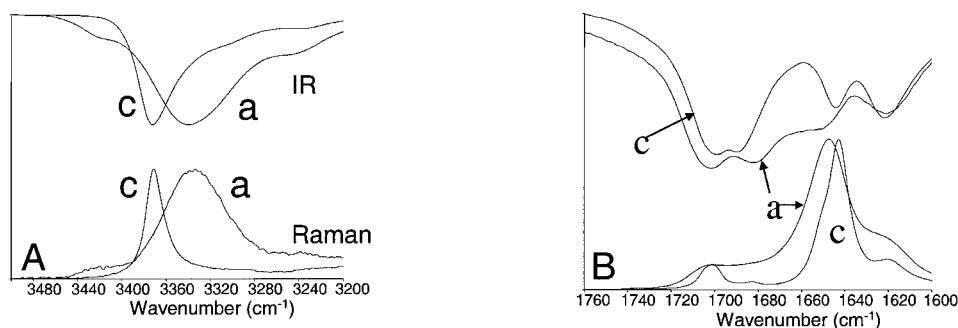


Fig. 4. Raman and IR spectra of crystalline and amorphous felodipine in the (A) NH and (B) C=O stretching regions. The crystalline sample is marked by a 'c' and the amorphous sample by an 'a'.

The spectra of isradipine also showed different strengths of hydrogen bonding in the crystalline and amorphous states. In the absence of published single crystal data, hydrogen bond patterns in the crystalline phase are postulated based on comparison with the other compounds. For crystalline isradipine, only one carbonyl peak is observed in the Raman/IR spectrum, at around 1700 cm^{-1} . This peak is thought to be composed of contributions from both carbonyl functions, and the high frequency indicates no hydrogen bonding occurs with these groups. We can thus speculate that in crystalline isradipine a hydrogen bond is formed with another functional group (most likely the benzoxadiazole ring), and this interaction is relatively weak because the stretching frequency of the NH group is quite high (3349 cm^{-1}) compared to the other compounds. In amorphous isradipine, the NH peak position has shifted downwards implying that, as seen for felodipine, hydrogen bonding is now stronger than in the crystalline counterpart. In addition, two carbonyl peaks are now observable, and a similar hydrogen bonding pattern as observed for the other amorphous compounds is proposed, i.e., whereby one of the carbonyl groups is involved in hydrogen bond formation.

Nicardipine was only available commercially as the HCl salt. This was converted to the free base, however, it was found to be difficult to obtain a fully crystalline sample. A partially crystalline sample was analyzed with IR and the NH peak was found to occur at a higher wave number (15 cm^{-1}) than for the fully amorphous sample, providing a further example of a compound where the hydrogen bonding appears to increase on changing from crystalline to amorphous. From Table II it can be seen that the NH position in amorphous nicardipine was very similar to the other amorphous compounds, as were the carbonyl peaks. Hydrogen bonding patterns for both forms are suggested in Table I.

DISCUSSION

Using spectral data we have been able to elucidate the hydrogen bonding strengths and patterns in a group of seven structurally related compounds by monitoring the NH stretching frequency. These NH peak positions are summarized in Fig. 5, where the compounds can be both contrasted with each other and a comparison between amorphous and crystalline counterparts made. Within the group of crystalline compounds, the extent of variation in NH peak position suggests a range of hydrogen bond distances and thus strengths, consistent with crystallographic data. A carbonyl group is the

preferred acceptor group for the majority of the crystalline compounds with the exception of nimodipine [which is unusual because carbonyls are usually favored over ether groups in hydrogen bonding (21)] and isradipine. Even excluding these two compounds, we can observe that there is a spread of approximately 50 cm^{-1} within a specific hydrogen bonding pattern. It is pertinent to consider what factors influence hydrogen bond strengths (and thus NH position). Undoubtedly, the largest influence is the chemistry of the donor and acceptor groups, which is relatively constant for the different compounds and cannot explain the observed variation. However, it has also been pointed out that most of the observed variations in hydrogen bond distances in crystalline materials are due to crystal packing (22). Brock and Dunitz consider the drive to maximize density and minimize free volume as the primary packing rule for crystals (1). We can thus speculate that in some of the crystal structures, the opportunity to maximize the hydrogen bonding interactions has been sacrificed for other packing factors. This speculation is supported by the hydrogen bonding in the amorphous compounds, discussed below.

In the amorphous materials, in contrast to the crystalline group, average hydrogen bond strengths appear to be very uniform, as shown in Fig. 5. There is a variation of less than 5 cm^{-1} for the NH peak position between the amorphous compounds compared to 70 cm^{-1} for the crystalline group.

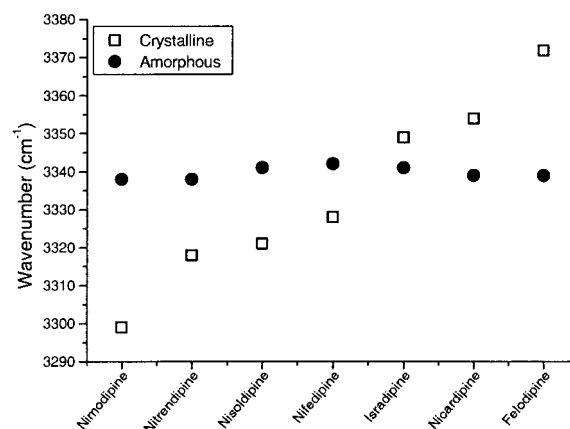


Fig. 5. A comparison of the NH stretching frequency for the compounds in the amorphous and crystalline states shows the significant variation for the crystalline compounds and a very uniform position for the amorphous materials.

Furthermore, the hydrogen bond pattern appears to be very consistent within the amorphous group, always between the NH and a carbonyl group, also indicating a change in motif for nimodipine and isradipine when comparing crystalline and amorphous phases. These observations suggest that since the chemistry of the donor and acceptor groups is very similar within this group of compounds, when the constraints of crystal packing are removed, very similar interaction patterns and strengths result. However, it should also be noted that in all instances, the width of the amorphous NH peak was greater than for the crystalline counterpart, which is consistent with a broader distribution of hydrogen bond lengths in the disordered phase. The hydrogen bonding in the amorphous state also appears to be quite selective—we only found evidence for interactions with carbonyl groups; other acceptor groups appear to be largely ignored. Self-association in a nonpolar solvent was also found to preferentially involve the carbonyl group as the acceptor group (data not shown). The observation that the carbonyl group is the preferred acceptor group can be rationalized if the relative basicities of the various acceptor functionalities are considered. These were calculated for nifedipine using the HYBOT software program (The MolPro Project Chernogolovka, Russia). The relative basicities of the carbonyl, nitro, and ether groups were found to be, 1.2, 0.48, and 0.12, respectively. Thus the carbonyl group is more than twice as basic as the nitro group. This suggests that to achieve the lowest energy state, the NH group should hydrogen bond in preference with a carbonyl group.

From Fig. 5, it is also apparent, perhaps somewhat surprisingly, that some of the compounds appear to have stronger average hydrogen bonding in the amorphous state than in the crystalline state, notably felodipine, nicardipine, and isradipine. For other compounds, the opposite situation was observed, and the hydrogen bonding weakens on changing from the ordered to the disordered state for nimodipine, nitrendipine, nisoldipine, and nifedipine. Few studies comparing crystalline and amorphous systems exist in the literature. In one study, an evaluation of hydrogen bond lengths in crystalline and amorphous glucose indicated there was an increase in average hydrogen bond length in the amorphous phase (3). We can speculate that a weakening of hydrogen bonding on progressing from an ordered to disordered phase is probably more typical than the converse.

On the basis of the above observations, it can be speculated that different energetic barriers exist for rearrangement within the amorphous phase prior to crystallization depending on the differences in molecular association between amorphous and crystalline phases, although clearly other factors such as molecular mobility have to be considered. Thus for felodipine, some hydrogen bonds have to be disrupted and/or weakened to crystallize and for nimodipine, bonds have to be both disrupted and reformed with another acceptor group. For other compounds, little rearrangement of hydrogen bonding is needed to achieve crystallization. Because a certain type of molecular association is needed to achieve crystallization, knowledge of how to disrupt the hydrogen bond patterns in amorphous compounds would presumably be useful as an aid to the physical stabilization of amorphous phases. Thus either donor and/or acceptor groups could be targeted to interact with polymeric crystallization inhibitors. Studies of molecular association in amorphous phases are complemen-

tary to molecular mobility investigations in understanding the behavior of and designing strategies to stabilize amorphous phases.

SUMMARY

Using a combination of IR and Raman spectroscopy, hydrogen bonding patterns and strengths have been investigated for a group of compounds in both the crystalline and amorphous states. For the crystalline group, both the pattern and the strength were found to differ considerably, and it was concluded that the observed variation is due to other packing factors. In contrast, for the amorphous group, both the hydrogen bond pattern and strength, as estimated from the NH peak position, was remarkably uniform. Furthermore, for some of the compounds investigated, the average hydrogen bond strength in the amorphous phase is greater than in the crystalline counterpart, whereas for most, a loss of crystallinity resulted in a decrease in hydrogen bond strength.

REFERENCES

1. C. P. Brock and J. D. Dunitz. Towards a grammar of crystal packing. *Chem. Mater.* **6**:1118–1127 (1994).
2. M. C. Etter. Encoding and decoding hydrogen-bond patterns of organic compounds. *Acc. Chem. Res.* **23**:120–126 (1990).
3. R. H. Tromp, R. Parker, and S. G. Ring. A neutron scattering study of the structure of amorphous glucose. *J. Chem. Phys.* **107**:6038–6049 (1997).
4. W. M. J. Risen. Optical spectra of glasses. *J. Non-Cryst. Solids* **76**:97–108 (1985).
5. J. F. Carpenter, M. J. Pikal, B. S. Chang, and T. W. Randolph. Rational design of stable lyophilized protein formulations: Some practical advice. *Pharm. Res.* **14**:969–975 (1997).
6. L. S. Taylor and G. Zografi. Spectroscopic characterization of interactions between pvp and indomethacin in amorphous molecular dispersions. *Pharm. Res.* **14**:1691–1698 (1997).
7. L. S. Taylor and G. Zografi. Sugar-polymer hydrogen bond interactions in lyophilized amorphous mixtures. *J. Pharm. Sci.* **87**:1615–1621 (1998).
8. P. C. Painter, Y. Park, and M. M. Coleman. Thermodynamics of hydrogen bonding in polymer blends. 1. The application of association models. *Macromolecules* **22**:570–579 (1989).
9. C. Doherty and P. York. Evidence for solid- and liquid-state interactions in a furosemide-polyvinylpyrrolidone solid dispersion. *J. Pharm. Sci.* **76**:731–737 (1987).
10. C. N. R. Rao and A. S. N. Murthy. Spectroscopic studies of hydrogen bonding. *Develop. Appl. Spectrosc.* **7B**:54–88 (1970).
11. D. Lin-Vien, N. B. Colthup, W. G. Fateley, and J. G. Grasselli. The Handbook of Infrared and Raman Characteristic Frequencies of Organic molecules. Academic Press, Inc., San Diego, California, 1991.
12. K. Nakamoto, M. Margoshes, and R. E. Rundle. Stretching frequencies as a function of distances in hydrogen bonds. *J. Amer. Chem. Soc.* **77**:6480–6486 (1955).
13. D. J. Skrovaneck, S. E. Howe, P. C. Painter, and M. M. Coleman. Hydrogen bonding in polymers: Infrared temperature studies of an amorphous polyamide. *Macromolecules* **18**:1676–1683 (1985).
14. G. A. Jeffrey. An Introduction to Hydrogen Bonding. Oxford University Press, New York, 1997.
15. A. M. Triggle, E. Shefter, and D. J. Triggle. Crystal structures of calcium channel antagonists: 2,5-dimethyl-3,5-dicarbomethoxy-4[2-nitro-,3-cyano-,4-(dimethylamino)-, and 2,3,4,5,6-pentafluorophenyl]-1,4-dihydropyridine. *J. Med. Chem.* **23**:1442–1445 (1980).
16. R. Fossheim. Crystal structure of the dihydropyridine ca²⁺ antagonist felodipine. Dihydropyridine binding prerequisites assessed from crystallographic data. *J. Med. Chem.* **29**:305–307 (1986).
17. S. D. Wang, L. G. Herbet, and D. G. Rhodes. Structure of the calcium channel antagonist, nimodipine. *Acta Cryst.* **C45**:1748–1751 (1989).

18. R. Fossheim, A. Joslyn, A. J. Solo, E. Luchowski, A. Rutledge, and D. J. Triggle. Crystal structures and pharmacological activities of 1,4-dihydropyridine calcium channel antagonists of the isobutyl methyl 2,6-dimethyl-4-(substituted phenyl)-1,4-dihydropyridine-3,5-dicarboxylate (nisoldipine) series. *J. Med. Chem.* **31**: 300–305 (1988).
19. A. Burger, J. M. Rollinger, and P. Bruggeller. Binary system of (R)- and (S)-nitrendipine - polymorphism and structure. *J. Pharm. Sci.* **86**:674–679 (1997).
20. R. C. Lord and R. E. Merrifield. Strong hydrogen bonds in crystals. *J. Chem. Phys.* **21**:166–167 (1953).
21. P. Murray-Rust and J. P. Glusker. Directional hydrogen bonding to sp² and sp³ hybridized oxygen atoms and its relevance to ligand macromolecular interactions. *J. Am. Chem. Soc.* **105**:5761–5766 (1983).
22. R. Taylor, O. Kennard, and W. Versichel. Geometry of the NH·O=C hydrogen bond. 3. Hydrogen bond distances and angles. *Acta Cryst.* **B40**:280–288 (1984).